Stability of spin states in quantum dots

S. Lindemann, T. Ihn, T. Heinzel,* W. Zwerger,† and K. Ensslin

Solid State Physics Laboratory, ETH Zürich, 8093 Zürich, Switzerland

K. Maranowski and A. C. Gossard

Materials Department, University of California, Santa Barbara, California 93106

We have investigated electronic transport through a Coulomb-blockaded quantum dot in which interactions are strong. Linear changes in conductance peak spacings with in-plane magnetic field are observed and interpreted in terms of Zeeman splitting of single-particle levels. Thereby, the measurements allow tracking changes in the dot's ground-state spin as the dot is gradually opened to the leads and the electron number is changed. Spin states have been identified in the weak- ($kT > \Gamma$), intermediate- ($\Gamma \approx kT$), and strong- ($\Gamma > kT$) coupling regime. It is found that ground states with spin $S = 0$ or $S = 1/2$ are most likely, while larger total spins $S \geq 1$ can occasionally occur, despite the large number of 50–100 electrons. A g factor close to the bare bulk GaAs value has been determined experimentally for the majority of the spin states. A perpendicular magnetic field applied to the dot in the same state allows the investigation of spin-pair candidates under conditions where orbital effects dominate the evolution of conductance peaks. Strong correlations in the position and in the amplitude of neighboring peaks allow the final identification of spin pairs. The method of combining parallel and perpendicular magnetic fields for identifying spin states and spin-pairs works well for intermediate and strong coupling of dot states to the leads while the data in the weak-coupling regime is less conclusive. Our results indicate that the spin degree of freedom is remarkably stable and the spin states are well described within a single-particle picture.

I. INTRODUCTION

The energy spectrum of quantum dots in semiconductor nanostructures can be investigated by Coulomb-blockade experiments.[1,2] For circularly symmetric few-electron quantum dots the measured energy spectrum directly reveals the shell structure of a zero-dimensional system.[3] In quantum dots containing 50 or more electrons the situation is more involved. The energy spectrum has been analyzed primarily on a statistical basis[4–7] and only in very exceptional cases the energy spectrum can be understood in detail.[8]

In addition to the energy spectrum, the spin of the ground state of tunable quantum dots is of fundamental interest.[9–13] In a picture of noninteracting electrons, each single-particle level is successively occupied by electrons with opposite spin according to the Pauli principle. While the Hartree interaction term has no direct influence on the ground-state spin, exchange effects favor the parallel alignment of spins and therefore tend to maximize the total spin of the ground state. The important parameter is the ratio of the interaction strength to the single-particle level spacing.[11] Recently it has been theoretically predicted that off-diagonal interaction fluctuations suppress the ground-state magnetization in finite size systems.[13] In many-electron systems with more than 50 electrons, exchange effects involving electron spin can become comparable to the single-particle level spacing Δ.[12] This is the reason why spin pairs, i.e., the successive population with spin-up and spin-down electrons in the same orbital state are expected to occur rarely. Experimentally, the effects of spin can be directly understood in certain few-electron quantum dots.[14–17] In many-electron dots based on GaAs/AlGaAs heterostructures the ratio of electron-electron interaction energy and Fermi energy $r_s = E_{ee}/E_F$ is typically of the order of 1 leading to very rare occurrence of spin pairs. For especially designed quantum dots, r_s can be significantly reduced and spin pairs are observed.[6–8]

Here we present a systematic study of quantum dots with a rather large r_s-value. The host electron gas is a parabolic quantum well[18] (PQW) with a suitably designed back-gate electrode.[19] The position of the electron gas in the growth direction can be tuned by front- and back-gate voltages.[20] Quantum dots have been realized on such PQW's using top-gate electrodes which are nanofabricated by electron-beam lithography.[21] Such systems have been investigated in the regime where the second subband for the confinement in the growth (z-) direction is occupied, and switching behavior of the Coulomb-blockade peaks has been observed, which can be attributed to the occupation of the second subband.[21] Here we focus on the regime where only one subband is occupied and switching events are absent. The quantum dots are as stable as those fabricated on regular two-dimensional electron gases (2DEGs) in heterostructures. With the back gate we drive the system to rather low densities $n_s < 1.5 \times 10^{15}$ m^{-2} such that $r_s \propto 1/\sqrt{n_s}$ can be as large as 1.5 as in Ref. 22 but smaller than in experiments on Si.[23]

Tuning the quantum dot into the Coulomb-blockade regime, we observe about 40 conductance peaks as a function of the plunger gate voltage. In this gate voltage interval we clearly see a transition from weak, to intermediate, and to strong coupling of the quantum dot to the source and drain, as indicated by a comparison of the Coulomb-blockade peak width with the single-particle level spacing.

Conceptually, our measurements are based on the spectroscopy of the addition spectrum of a quantum dot in the

Coulomb-blockade regime. It is well accepted that spin-orbit coupling in the conduction band of GaAs/AlGaAs structures is neglibible and therefore the total energy of the N-electron quantum dot state in a magnetic field B is the sum of an orbital contribution $E_N(B)$ and a spin contribution $E_S(B) = s_N g \mu_B B$, where s_N is the component along the direction of B of the total spin of the quantum dot. Peaks in the conductance will be observed for plunger gate voltages

$$V_{pg}^{(N+1)}(B) = \frac{1}{e \, \alpha_{N+1}} [E_{N+1}(B) - E_N(B)$$
$$+ (s_{N+1} - s_N) g \mu_B B], \qquad (1)$$

where $\alpha_{N+1} \equiv \alpha$ is the electrostatic lever arm of the plunger gate which depends typically very weakly on the electron number N. The differences $(s_{N+1} - s_N)$ can, in principle, take on values $\pm 1/2, \pm 3/2, \ldots$. In a single-particle picture, the difference of the orbital energies can be expressed as

$$E_{N+1}(B) - E_N(B) = \epsilon_{N+1}(B) + U_{N+1}^H(B) + U_{N+1}^{xc}(B), \qquad (2)$$

where $U_{N+1}^H(B)$ is the Hartree energy, $U_{N+1}^{xc}(B)$ is the exchange energy, and $\epsilon_{N+1}(B)$ is the confinement energy of the $(N+1)$th electron.

For magnetic fields $B_\parallel$ applied in the plane of the 2DEG we observe a pronounced shift of the Coulomb-blockade peaks similar to previous experiments.[24,25] The main contribution to this shift is due to the relative diamagnetic shift of energy levels $\epsilon_N(B_\parallel)$ in the dot, which has a $B_\parallel^2$ dependence. We will show below (see Sec. VI) that it is the same for all conductance peaks. It can therefore be eliminated by analyzing peak separations $\Delta V_{pg}^{(N+1)}(B_\parallel) = V_{pg}^{(N+1)}(B_\parallel) - V_{pg}^{(N)}(B_\parallel)$ rather than the absolute peak positions, if the reasonable assumption is made that the interaction energies are independent of $B_\parallel$. We find experimentally that for most conductance peaks in all coupling regimes, the Coulomb peak separation is either constant or changes linearly in $B_\parallel$. This can be explained on the basis of Zeeman splitting of the dot levels, since according to Eqs. (1) and (2) and the assumptions mentioned above,

$$e \, \alpha_{N+1} \Delta V_{pg}^{(N+1)}(B_\parallel) = (s_{N+1} - 2s_N + s_{N-1}) g \mu_B B_\parallel + \text{const.} \qquad (3)$$

Plotting $e \alpha V_{pg}^{(N+1)}$ versus $B_\parallel$ will according to this equation show branches with slopes $0, \pm g \mu_B, \pm 2 g \mu_B, \ldots$. We will show experimentally that mainly the three slopes $0, \pm g \mu_B$ are observed.

The Zeeman splitting for all magnetic fields investigated is much smaller than the Fermi energy in source and drain. We therefore expect that Zeeman effects in source and drain can be neglected and that both spin directions are available for tunneling through the dot at all magnetic fields. If differences of certain neighboring conductance peak positions display a linear magnetic field dependence, we interpret such shifts as arising entirely from the Zeeman effect in the quantum dot.

When the sample is rotated *in situ*, i.e., without warming it up, from the parallel to the perpendicular magnetic field direction, the dot spectrum at $B = 0$ is basically left unchanged. In this perpendicular case the peak movement with $B_\perp$ is dominated by orbital effects via $\epsilon_N(B_\perp)$ and the Zeeman term in Eq. (1) is negligible. We find that about every tenth pair of neighboring peaks shows correlated behavior of amplitude and position. This unique combination of in-plane and perpendicular fields applied successively to a quantum dot in the same state allows a comparison of the dot's energy spectrum and spin splitting over wide ranges of electron number and dot-lead coupling. The results for intermediate coupling can be satisfactorily discussed in terms of a single-particle picture, which essentially assumes the absence of any coupling between the spin and the orbital degrees of freedom. Deviations from such a description are observed for weak and strong coupling.

II. EXPERIMENT

The quantum dot samples are based on molecular-beam-epitaxy-grown parabolic $Al_x Ga_{1-x} As$ quantum wells with x varying parabolically between 0 and 0.1.[18,20] The 760-Å-wide wells are sandwiched between 200-Å-thick undoped $Al_{0.3} Ga_{0.7} As$ spacer layers and remotely doped with Si on both sides. A 3-ML-thick $Al_{0.05} Ga_{0.95} As$ layer in the center of the well leads to a potential spike which is used to monitor the position of the wave functions with respect to the parabolic confinement.[20] However, this spike is not relevant for the present study. A back-gate electrode consists of a 150-Å-thick n^+-doped layer located 1.35 μm below the well. Using the back-gate electrode the density of the 2DEG in the PQW can be varied from $n_s = 1 \times 10^{15}$ m^{-2}, where only one subband is occupied in the well, up to 5×10^{15} m^{-2}, where three subbands are occupied. In this density range the mobility changes from 8 m^2/V s at the lowest to 14 m^2/V s at the highest densities. The occupation of the second subband starts at $n_s = 2.4 \times 10^{15}$ m^{-2}.

The inset in Fig. 1 shows the TiAu top-gate electrodes fabricated using electron-beam lithography and a lift-off process. These electrodes define a lateral quantum dot with geometric lateral dimensions of 600 nm × 600 nm connected to source and drain contacts via the two quantum point contacts (QPC's) QPC1 and QPC2. Two plunger gates allow tuning the number of electrons in the quantum dot by varying the plunger gate voltage V_{pg}. DC-conductance measurements were carried out with an applied source-drain voltage $V_{SD} = 8$ μV at an electron temperature of less than 140 mK in a dilution refrigerator.

The sample is mounted on a revolving stage. For in-plane fields we measure the Hall effect of the underlying 2DEG in order to make sure that the angle is accurate to within 0.01°. This means that less than one tenth of a flux quantum threads the area of the dot for in-plane fields as high as 13 T. The perpendicular field direction can only be determined with about 0.3° accuracy, which is enough since orbital effects on the Coulomb-blockade peak position are about two orders of magnitude stronger than spin effects.

The sample has been studied for a wide range of back-gate voltages. Here we focus on a rather large negative value, $V_{bg} = -4.5$ V, where the density of the 2DEG is $n_s = 1.5$
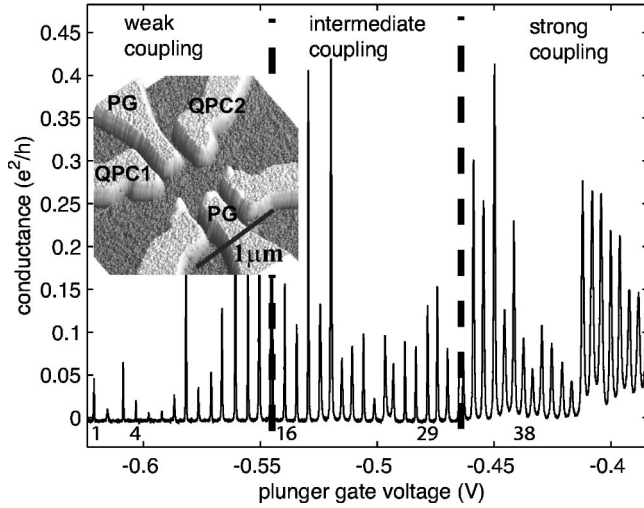
FIG. 1. Coulomb-blockade conductance peaks versus plunger gate voltage taken at $B_{total}=0$ and with a back-gate voltage $V_{bg}=-4.5$ V. The numbers at the bottom of the figure are used to identify peaks. This numbering is used throughout the paper. The vertical dashed lines divide the data into three regimes, namely, weak, intermediate, and strong coupling. The inset in the upper left shows a scanning force microscope image of the surface gates defining the quantum dot. Two pairs of gates (QPC1 and QPC2) form the entrance and exit quantum point contacts. A pair of plunger gates (PG) allows to tune the electron number in the dot.

$\times 10^{15}$ m^{-2}. At these low electron densities, it is the tunability of the dot via the back gate which is crucial for the presented experiments rather than the special parabolic confining potential of the quantum well.

With the QPC's in the tunneling regime the Coulomb-blockade effect could be observed as depicted in Fig. 1. From an analysis of the Coulomb-blockade diamonds measured in the V_{pg}-V_{SD} plane[26] for the weak-coupling regime (see Fig. 2) we determine a charging energy of about
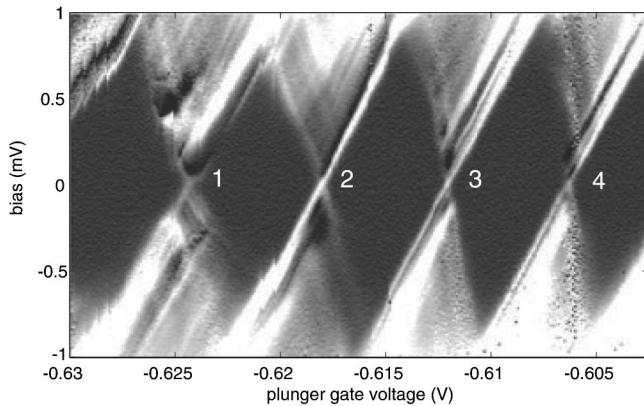

FIG. 2. Differential conductance for $B_{total}=0$ in a gray scale plot showing Coulomb-blockade diamonds. Black corresponds to zero conductance, white regions represent conductances above 10^{-6} Ω^{-1}. The addition energy (between peak 2 and 3) extracted from these measurements is 920 μeV, the single-particle level spacing is about 100 μeV, and the lever arm $\alpha=C_g/C_\Sigma=0.155$, relating plunger gate voltage to energy.

920 μeV. Using the self-capacitance of a circular disk, $C_\Sigma=8\varepsilon\varepsilon_0 r$, we find a dot radius of $r=190$ nm. This agrees well with the geometrical size if a reasonable depletion length of 100 nm is taken into account. From this dot size the average single-particle level spacing can be estimated to be $\Delta=2\pi\hbar^2/(m^\star\pi r^2)\approx 60$ μeV assuming spin degeneracy of the levels. This value is in rough agreement with the evaluation of transport through excited states (see Fig. 2), which gives a value of about 100 μeV. Further details of the Coulomb diamonds in Fig. 2 are beyond the scope of this paper.

In order to determine the 2D electron density n_d in the dot, which is typically smaller than the density in the unbound 2DEG at the same back-gate voltage, we analyzed magneto-Coulomb oscillations[27] as a function of V_{pg}. All top-gate voltages have to be readjusted when V_{bg} is significantly changed in order to stay in the Coulomb-blockade regime. A more positive V_{bg} will pull the electron distribution in the well towards the back gate. As a consequence, the front-gate voltages have to be decreased in order to establish the necessary conditions for the observation of Coulomb blockade again (for details see Ref. 21). From such measurements we estimate the 2D density in the dot to be around $n_d=0.5\times10^{15}$ m^{-2} for the smallest plunger gate voltages, which leads to about 50 electrons populating the dot. These numbers are confirmed by the $\nu=2$ line at about $B=1.05$ T (see Fig. 7).[15,16]

The experimental trace in Fig. 1 covers a range of about 40 Coulomb-blockade maxima, i.e., the dot population changes by about 40 electrons. In this range the coupling of the dot to its leads quantified by the width Γ of the conductance peaks, changes significantly due to capacitive cross talk between the plunger gate and QPC's. We have identified three regimes, named weak, intermediate, and strong coupling. These regimes are marked in Fig. 1 and separated by vertical dashed lines. The exact position of the boundaries between weak, intermediate and strong coupling can be chosen somewhat arbitrarily. The coupling strength is used as a parameter to distinguish the three regimes. Qualitatively, in the weak-coupling regime conductance peaks are thermally broadened ($kT>\Gamma$), in the intermediate-coupling regime we have $\Gamma\approx kT$, and in the strong-coupling regime $\Gamma>kT$. The numbering of the Coulomb-blockade maxima in Fig. 1 is kept consistent throughout this paper. Obviously, also the electron number is different in the three coupling regimes.

A careful analysis of Coulomb charging energy, single-particle level spacing, and dot size has been performed for all regimes and is summarized in Table I. The capacitance $C_\Sigma=e^2/E_c$ cannot easily be translated into the geometric dimensions of the dot. The model of the self-capacitance of an isolated two-dimensional disk tends to overestimate the dot radius. As mentioned before, we estimate $\Delta\approx 60$ μeV assuming a circular dot shape for weak coupling. In this regime the conductance peaks are thermally broadened and their width Γ is independent of gate voltage. The fact that $\Gamma<\Delta,kT$ indicates that we are close to single-level transport. However, when the dot is opened, the width of the conductance peaks is no longer determined by thermal broadening but increases with increasing gate voltage due to the in-

TABLE I. Parameters of the dot in the different coupling regimes as classified by the width of conductance peaks. The Coulomb peaks have been fitted based on thermal smearing. In the weak-coupling regime, the width of the peaks is governed by temperature, leading to the value $T = 142$ mK. In the intermediate- and strong-coupling regimes the width of the peaks is more and more determined by the tunneling coupling Γ. The Coulomb energy $\langle E_C \rangle$ is extracted from Coulomb diamonds and the mean peak spacing $\langle \Delta V_g \rangle$ from plunger gate sweeps at $B = 0$ T. The quantity $\langle g \rangle$ is the average conductance peak height, $\langle \alpha \rangle = C_{pg}/C_\Sigma$ is the electrostatic lever arm of the plunger gate. The typical number of electrons $\langle N \rangle$ is determined from the sheet electron density in the dot (see text) and the dot size for the weak-coupling limit. Counting conductance peaks leads to the typical electron numbers for the other two regimes.

	Coupling		
Parameter	Weak	Intermediate	Strong
Peak width	43 μeV (142 mK)	52 μeV	83 μeV
$\langle g \rangle$	$0.04e^2/h$	$0.14e^2/h$	$0.18e^2/h$
$\langle E_C \rangle$	920 μeV	625 μeV	400 μeV
$\langle \Delta V_g \rangle$	5.8 mV	4.7 mV	4.2 mV
$\langle C_\Sigma \rangle$	174 aF	256 aF	400 aF
$\langle \alpha \rangle$	0.159	0.133	0.095
$\langle N \rangle$	~ 50	~ 70	~ 90

creased dot-lead coupling. At the same time, the dot size increases and the single-particle level spacing decreases. In the strong-coupling limit we have $\Delta \sim \Gamma$ and observe a finite conductance between conductance peaks.
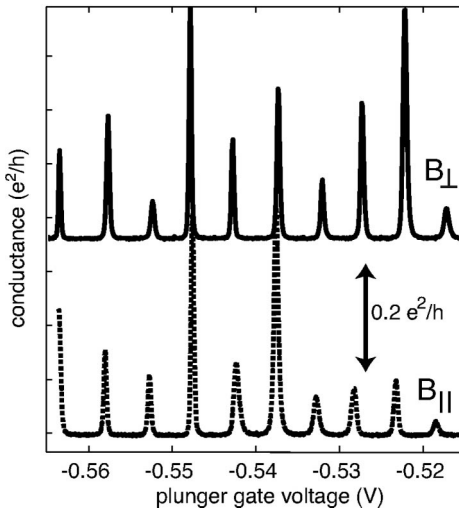

FIG. 3. Coulomb peak resonances measured for the intermediate-coupling regime at $B_{total} = 0$ before and after rotating the sample *in situ*. Rotating leads to a slight temporary heating due to mechanical friction, but the sample never warms up above 500 mK. Data is taken after equilibration to base temperature. The labels $B_\perp$ and $B_\parallel$ refer to the direction of magnetic field once applied. The two curves have been laterally offset by 17 mV and vertically offset for clarity. The peak amplitudes are slightly different while the peak positions suggest that the quantum states keep their specific character upon rotation of the sample.
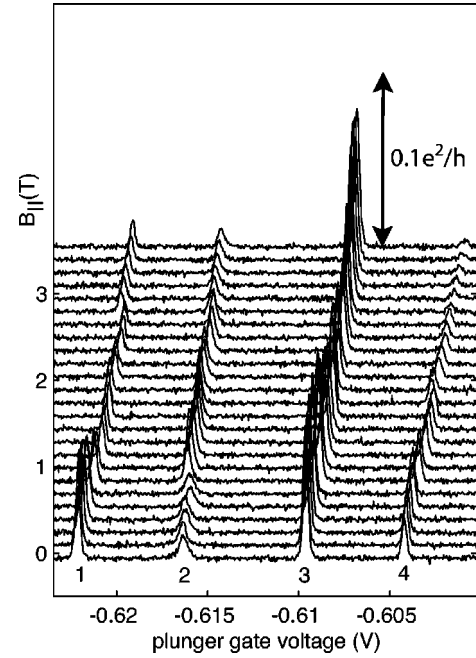

FIG. 4. Conductance through the quantum dot as a function of plunger gate voltage and in-plane magnetic field $B_\parallel$ in the weak-coupling regime. The magnetic field $B_\parallel$ is increased from 0 to 3.6 T in steps of 50 mT and the plunger gate is swept in steps of 40 μV. Only every third measured curve is shown.

Figure 3 shows two plunger gate sweeps before and after the sample has been rotated by 90°. The rotation creates friction and therefore warms the mixing chamber temporarily to about 500 mK. The basic Coulomb-blockade behavior is, however, recovered after rotation and we are confident that we look at the same dot, i.e., the same energy spectrum.

III. WEAK-COUPLING REGIME

We first focus on data taken in the weak-coupling regime. Figure 4 shows the conductance through the quantum dot as a function of plunger gate voltage for a series of parallel magnetic fields $B_\parallel$. The movement of the peak positions with magnetic field is clearly visible. The graph also demonstrates that the sample is stable over the duration of the experiment, i.e., there are no serious charge rearrangements over the course of about 24 h. This is a precondition for measurements of such small effects as the Zeeman splitting.

Figure 5(a) presents spacings of neighboring Coulomb peaks. As mentioned before, the lever arm relating plunger gate voltage to energy in the dot is extracted from the measured Coulomb diamonds[26] in Fig. 2. The change of lever arm with plunger gate voltage is explicitly taken into account. The curves are relatively flat up to magnetic fields of about 0.8 T. With the bare g factor of GaAs, $g = -0.44$, the Zeeman splitting is about $E_Z = |g|\mu_B = 25$ μeV/T. The electron temperature as determined from the Coulomb-blockade peak width of $3.5kT = 42$ μeV results in $T \approx 140$ mK. As long as the Zeeman splitting is small compared to thermal smearing, one does not expect a Zeeman shift. Only when the Zeeman splitting exceeds thermal smearing, a single spin
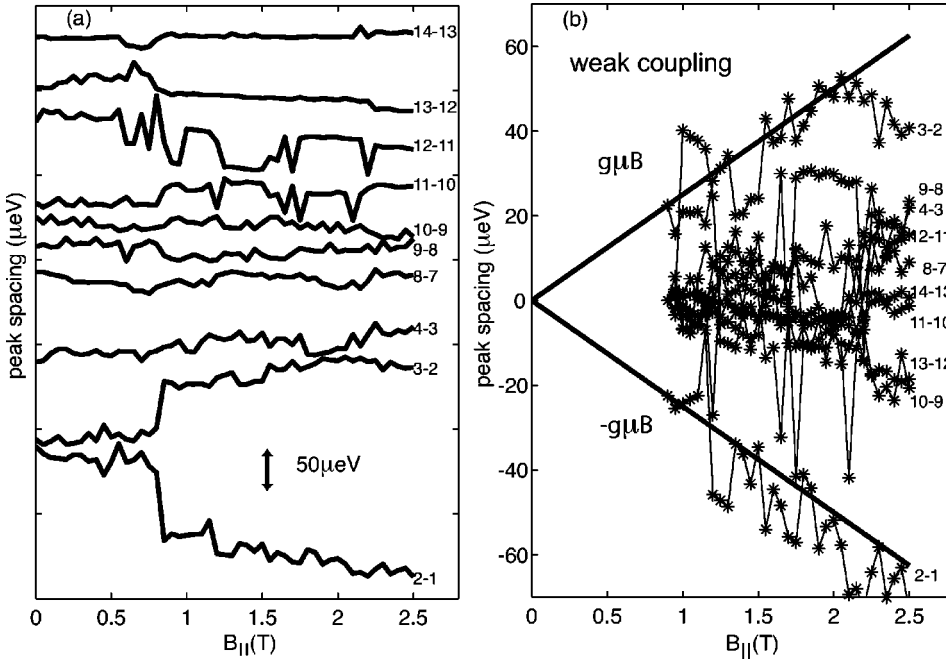
FIG. 5. (a) Evolution of peak spacing of the weak-coupling regime with in-plane magnetic field. The peak spacing is extracted from the measured peak motion (see Fig. 4), converted into energy using the lever arm α from the nonlinear conductance measurements of Fig. 2, and vertically offset for clarity. (b) Peak spacings offset to align spacings at $B_{\parallel} = 0$ T and converted into an energy using the corresponding lever arm α extracted from the Coulomb diamonds. The slope vs B corresponds to the change in ground-state spin as each electron is added and hence indicates the change of the spin from one state to the other. The straight lines show the slope as expected for the bulk GaAs g factor $|g| = 0.44$.

level dominates the conductance peak, which then shifts in accordance with this level. This explains why the Zeeman splitting can only clearly be observed at magnetic fields above 1 T, where the Zeeman splitting is larger than kT. All the peaks have been fitted to a thermally broadened line shape in order to obtain the peak positions most precisely. The effects of g-factor tuning as observed in Ref. 28 are not relevant for the present sample design.

We often observe an abrupt change in peak position at $B \approx 0.8$ T (see Fig. 5). Background charge rearrangements are a very unlikely cause for these effects since only some peaks are affected and not the entire spectrum. A possible reason could be exchange effects, which could suddenly set in once the Zeeman gap exceeds kT in a bootstrap effect. However, the magnitude of the jump as well as the extrapolation of the high-field behavior of peak separation down to $B = 0$ do not support this hypothesis.

It is important to note that in this weak-coupling regime only peak spacing 2-1 and 3-2 follow roughly the expected slope for a Zeeman energy shift, $-g\mu_B$ and $+g\mu_B$, respectively. Disregarding the strong peak spacing fluctuations, all the other peak spacings show a more or less flat behavior or slopes corresponding to a value less than expected for Zeeman splitting. This behavior would agree with the notion that in a closed few-electron dot, subsequent levels are preferentially filled with parallel spins in analogy to Hund's rules for atoms. Only very rarely, neighboring peaks correspond to opposite spins (see peaks 3-2 and 2-1). However, as mentioned above, we observe strong peak spacing fluctuations as a function of parallel magnetic field (see Fig. 5) as also reported in Ref. 25. We have no detailed understanding of these fluctuations but speculate that the ground state of the dot may be changed due to correlation effects as a function of parallel magnetic field causing the observed behavior.

IV. INTERMEDIATE COUPLING

Figure 6(a) shows the positions of Coulomb-blockade peak spacings versus parallel magnetic field in the intermediate-coupling regime. The curves are vertically offset for clarity. Again, peak spacings do not change below about 1 T and then gradually acquire their linear slope. At higher fields all curves show a linear magnetic-field dispersion. This is more clearly seen in Fig. 6(b), where the curves are offset to a common origin at $B = 0$. The straight lines are calculated with the bulk g factor of GaAs. The curves fall into three classes, namely, those with a negative slope, a positive slope, or a flat behavior. Very similar behavior was observed for GaAs (Refs. 24 and 25) and Si (Ref. 29) quantum dots.

Flat behavior is expected if successive electrons with the same spin occupy successive orbital states. It is possible to define a population sequence of single-particle spin states $s_{N+1} - s_N$ [see right-hand column in Fig. 6(a) and cf. Eq. (3)] similar to what has been done in Ref. 25. In this case the sequence is $\uparrow\downarrow\uparrow\downarrow\downarrow\downarrow\uparrow\uparrow\downarrow$ for levels 21–30. This sequence is consistent with the experimental observation as presented in Fig. 6(b) [cf. Eq. (3)]. Neighboring levels which are populated with opposite spins are possible candidates for spin pairs, i.e., states with the same orbital wave functions. Using Eq. (3) we can work out possible sequences of ground-state spins s_N of the quantum dot. Although there is more than one sequence compatible with the experiment, we can state that for the most probable sequences, i.e., those for which the maximum $|s_N|$ is kept as small as possible, about 80% of the ground states have $|s_N| = 0$ or 1/2, while the remaining fraction has $|s_N| = 1$.

In Fig. 7(a) we present Coulomb peak maxima versus perpendicular magnetic field $B_\perp$. Spin effects due to Zeeman splitting are expected to be of minor importance for this magnetic-field orientation. The movement of the energy levels is rather governed by orbital effects and level crossings. The correspondence of peaks after sample rotation is shown in Fig. 3. Peak amplitudes are shown in Fig. 7(b).

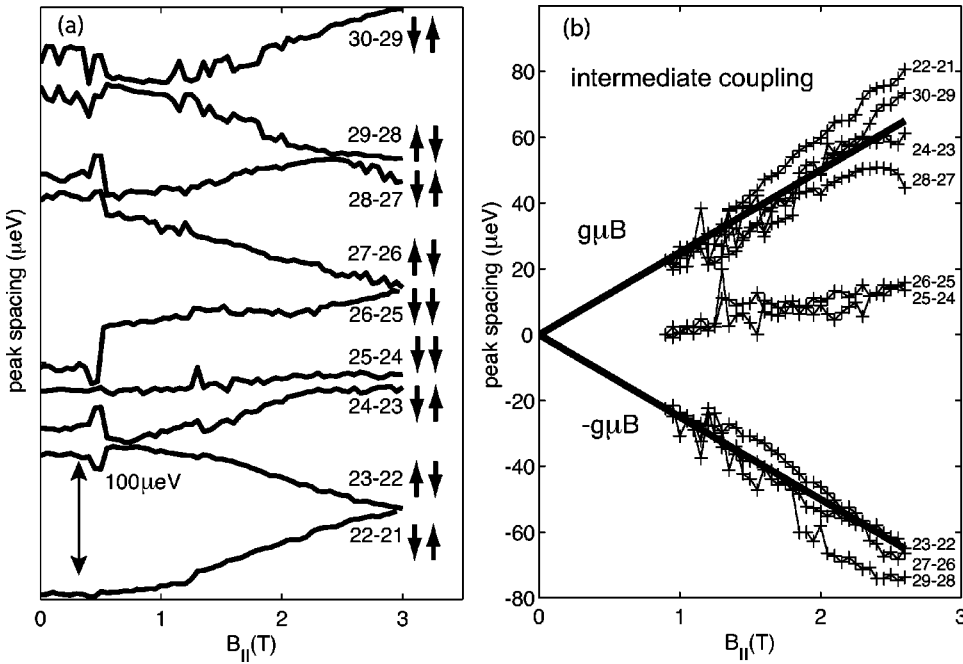We can identify pairs of peaks, namely, peaks 28 and 29

FIG. 6. (a) Evolution of peak spacing of the intermediate-coupling regime with in-plane magnetic field. The peak spacing is extracted from the measured peak motion (not shown here), converted into energy using the lever arm α, and shifted together in arbitrary units. The peak spacing is in most cases flat up to a magnetic field of about 0.8 T (see text for details). (b) Peak spacings are offset such that the lines cross at $B_\parallel = 0$ T.

as well as 27 and 26, whose position and amplitude dependences are strongly correlated in the magnetic-field range from 0.25 to 1.25 T. We have confirmed this by calculating the cross correlation of amplitude and position between these peaks. For the parallel field data, these peak pairs show a linearly decreasing peak separation [see Fig. 6(a)], in tune with the interpretation that the same orbital level is successively populated by spin-up and spin-down electrons. The combined measurement of the same dot in parallel and perpendicular field has enabled us to identify spin pairs in a strongly interacting dot, e.g., neighboring conductance peaks that are governed by transport through the same orbital state with alternating spin.

For magnetic fields where the filling factor in the dot is $\nu < 2$, the Coulomb-blockade maxima are known to shift smoothly as a function of perpendicular field (see, e.g., Ref. 30). In this way we identify the position of $\nu = 2$ in Fig. 7 and find good agreement with the previously mentioned carrier density in the dot.

At magnetic fields just below the $\nu = 2$ feature there is an odd-even behavior, i.e., the peak position shows an upward cusp for peaks 22, 24, 26 and a flat behavior for peaks 21, 23, 25, and 27 (see the four downward arrows in Fig. 7). Similar features have been reported before[30] and could be related to ground-state spin rearrangements in the dot.

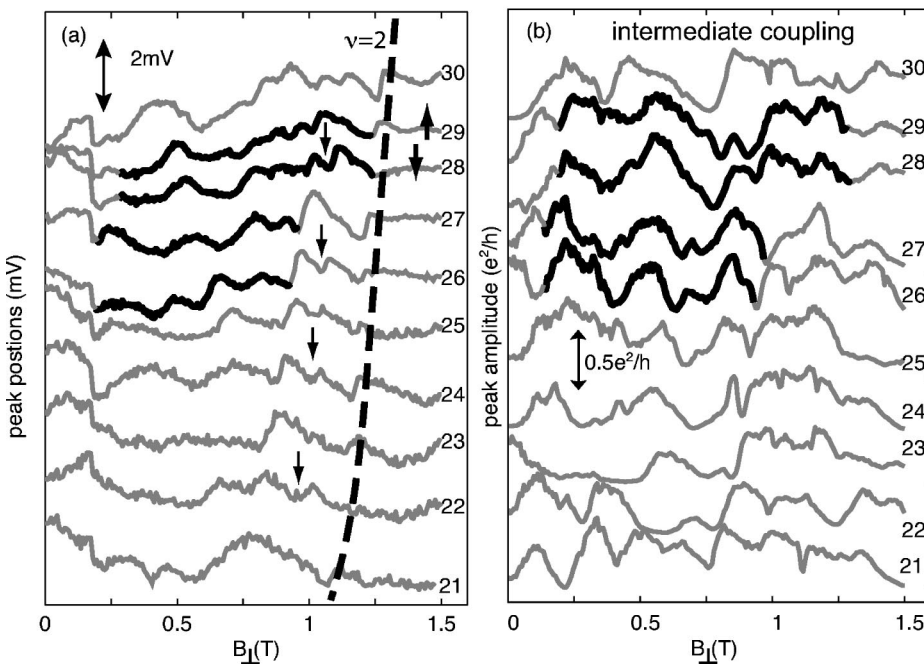The Coulomb peaks in the intermediate-coupling regime

FIG. 7. (a) Parametric variation of the peak position in a magnetic field perpendicular to the 2DEG for ten consecutive Coulomb-blockade peaks. Consecutive peaks are offset by 4.1 mV. Also indicated is the $\nu = 2$ line. (b) Parametric evolution of the peak conductance, vertically offset by $0.5e^2/h$ with respect to each other. A pair correlation in peak position and peak amplitude is clearly visible for peaks 26 and 27 as well as for 28 and 29 (black lines), suggesting that the respective electrons occupy the same orbital state forming a singlet.
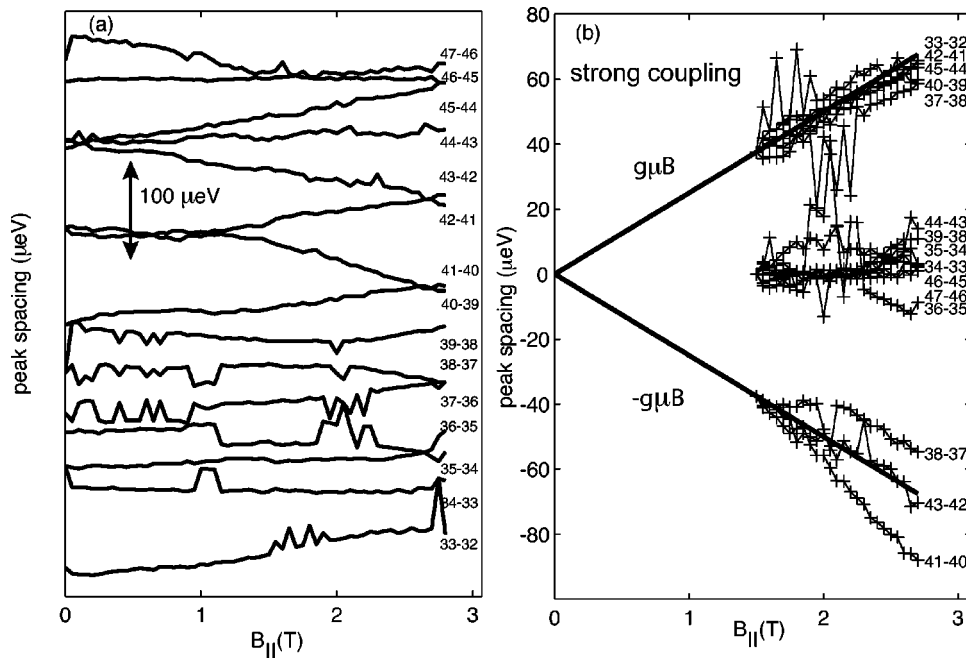
FIG. 8. (a) Evolution of peak spacing (strong-coupling regime) with in-plane magnetic field. (b) Peak spacings offset to align spacings at $B_\parallel = 0$ T and converted into energy using the corresponding lever arm α extracted from the Coulomb diamonds.

follow the behavior expected from the single-particle picture outlined in the Introduction [see Eqs. (1)–(3)]. Although we expect that in the intermediate-coupling regime more than one dot level contributes to the individual conductance peaks due to level broadening, the transmission of spin-up and spin-down electrons as a function of energy are essentially independent in this case. One could then expect independent Zeeman shifts of these transmission functions in opposite directions, leading exactly to the observed behavior.

V. STRONG COUPLING

For more positive plunger gate voltages ($V_g > -0.47$ V in Fig. 1) the conductance of the dot increases and the dot becomes strongly coupled to the leads. We first present the Coulomb peak spacing versus parallel magnetic field in Fig. 8. Again the traces roughly fall into three categories, namely, linear up or down movement in the magnetic field and flat curves almost independent of the magnetic field. On the right-hand side in Fig. 8(b) the theoretical expectation based on the bulk g factor of GaAs is plotted in the same graph. There are clear deviations from these lines, namely, peak spacing 41-40 actually displays a larger slope than expected. Especially for back-gate sweeps (not shown) we find many peak spacing slopes strongly exceeding the expected Zeeman splitting.

Trying to extract possible sequences of ground-state spins s_N like we did in the intermediate-coupling regime, we have been successful for peaks 34–47 with the result that 85% of all ground states have spin $|s_N| = 0$ or 1/2 and the rest is $|s_N| = 1$. Including peaks 32 and 33 in the analysis leads to unreasonably high spin states up to 7/2. We also find it impossible to obtain a reasonable sequence for the intermediate- and strong-coupling regime combined. The occurrence of ground-state spins $S > 1$ seems to be unreasonable for our dot with 50–100 electrons. Therefore, one could ask whether there are other mechanisms that can disturb the

sequence of experimental peak shifts. One possible scenario could be that occasionally the ground-state spin of the dot changes parametrically with the plunger gate voltage *within the Coulomb blockade*, i.e., in the valley between two conductance peaks. Such a change could not be detected but would lead to unrealistic sequences of spin states when determined according to Eq. (3). However, from the fact that our analysis works well for sequences of 10–15 conductance peaks, we are confident that such irregularities are the exception rather than the rule.

Peak position and amplitude are plotted as a function of perpendicular field in Fig. 9. The behavior is erratic and no clear spin pair (with the possible exception of peaks 37 and 38) can be detected. The calculated cross correlation in position is high for all neighboring peaks. This behavior is in accordance with the expected mesoscopic conductance fluctuations in the strong-coupling regime,[31] implying that strong level mixing occurs.

Summarizing, even in this strong-coupling regime, the peak spacings in parallel field still collapse reasonably well onto the three branches expected from the single-level transport picture. The rare occurrence of larger slopes remains an issue to be addressed in the future.

VI. DIAMAGNETIC SHIFT

For large parallel magnetic fields the energy levels in the dot as well as those in the leads are shifted up by the diamagnetic shift.[32] All previous data in this paper were shown as a function of plunger gate voltage. In order to present a comprehensive set of data we show the behavior as a function of back-gate voltage in Fig. 10.

One expects that the energy levels would follow a parabolic field dependence.[32] The parallel magnetic field is applied along the direction of current flow through the single-electron transistor. For 2DEG's in parabolic quantum wells with similar parameters as that investigated in this study,
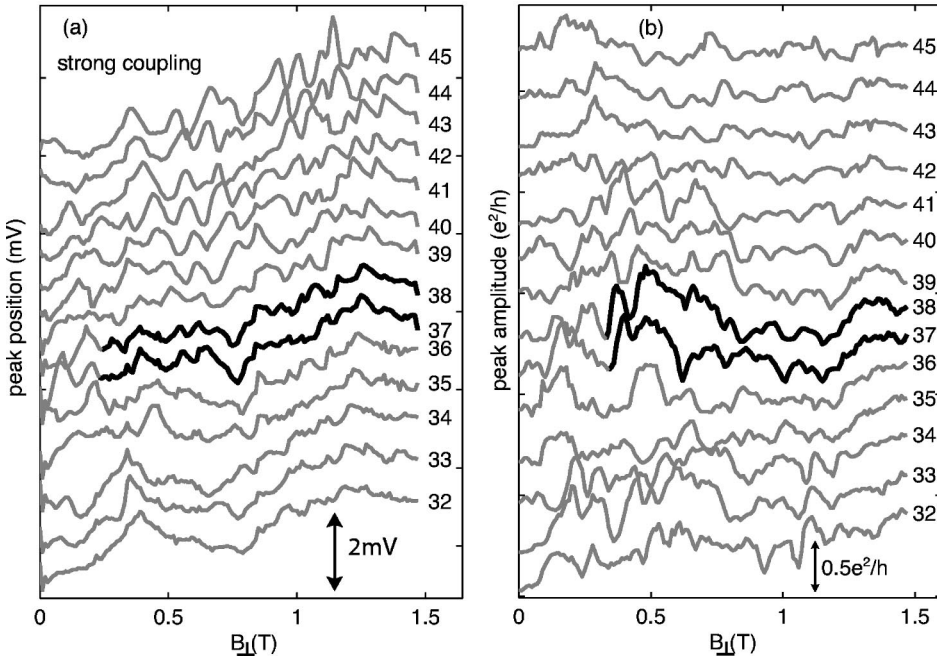
FIG. 9. (a) Parametric variation of the peak position (strong-coupling regime) in a magnetic field perpendicular to the 2DEG for 14 consecutive Coulomb-blockade peaks. Consecutive peaks are offset by 3.5. (b) Parametric conductance amplitude of the same peaks, offset by $0.4e^2/h$ each. Significant pair correlation in peak position and peak amplitude is visible for peaks 14 and 13 (black lines), suggesting they occupy the same orbital state.

such experiments have been done and analyzed in detail.[33] Here the situation is more involved since the energy levels in the quantum dot are confined in both directions perpendicular to the magnetic field. The energy levels in the source and drain also undergo a diamagnetic shift, and the net shift of conductance peaks will result from differences in the shift in the dot with respect to the source and drain. Since all effects are expected to be parabolic in the magnetic field, the overall behavior as observed in Fig. 10 is in tune with this picture.

The data indicate that the diamagnetic shift in the quantum dot is stronger than in the surrounding 2DEG, i.e., the Coulomb peak positions move up in gate voltage with increasing in-plane magnetic field. For a perfect parabolic po-

tential one would expect that the lower the Fermi energy is, the narrower is the wave function and therefore the smaller is the diamagnetic shift. In our case a very negative back-gate voltage is applied, which pushes the wave function in the z direction towards the hard wall which delimits the parabolic potential. In this case the behavior is reversed because a higher Fermi energy leads to a steeper potential via the Hartree interaction and therefore to a narrower wave function. We have simulated the parabolic potential self-consistently and indeed find the two trends in the two regimes as described above. The effectively positive diamagnetic shift as observed in the data of Fig. 10 can thus be explained by the wave function probing the hard edges of the parabola in the z direction. Indeed we find that for more positive back-gate voltages and therefore larger carrier densities in the parabolic quantum well, where the electrons reside more in the center of the parabola, the general shift of the Coulomb peaks with magnetic field is reversed (not shown).

For a more quantitative analysis we use the following model. The confinement potential of the dot in the y (in-plane) and z (growth direction) directions is modified by a magnetic field along the x direction (direction of current flow in the plane). The potential in these two directions is approximately parabolic and we can write

$$V(y,z) = \frac{1}{2}m^\star \omega_y^2 y^2 + \frac{1}{2}m^\star \omega_z^2 z^2.$$

The potential in the z direction is given by the as-grown parabola including its hard wall boundaries and modified by electron-electron interactions. The bare potential in the y direction is produced by the voltages applied to the gate electrodes. Obviously, the sample is in the limit $\omega_y \ll \omega_z$. The Schrödinger equation with the above potential and a magnetic field applied along the x direction can be solved analytically. The resulting energy spectrum is
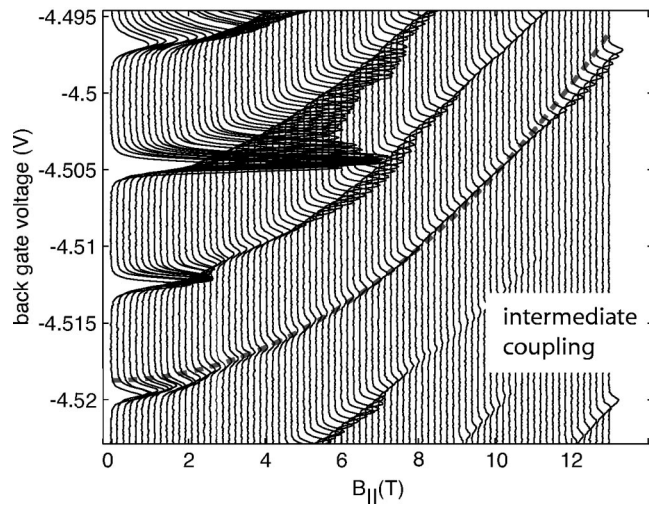

FIG. 10. Coulomb-blockade resonances as a function of back-gate voltage and parallel magnetic fields in the high-field range. The plunger gate voltage was $V_{pg} = -0.525$ V, i.e., in the intermediate-coupling regime. The dashed line is a parabolic fit as described in the text.

$$E_{n,l} = \hbar\omega_1\left(n + \frac{1}{2}\right) + \hbar\omega_2\left(l + \frac{1}{2}\right),$$

where ω_1 and ω_2 are functions of ω_y, ω_z, and $\omega_c = eB/m^\star$. For small magnetic fields $B < 5$ T, where $\omega_c \ll \omega_z$ we find

$$\omega_1 \approx \sqrt{\omega_z^2 + \omega_c^2} + O(\omega_y^2/\omega_z^2),$$

$$\omega_2 \approx \omega_y + O(\omega_y^2/\omega_z^2).$$

The dominant contributions to the diamagnetic shift originate from the strong confinement ω_z in the z direction, while the orbital effects governed by the weak confinement ω_y are of order $(\omega_y/\omega_z)^2$. Since $(\omega_y/\omega_z)^2 = (l_z/l_y)^4 \approx 10^{-4}$, with $l_{y,z}$ being the corresponding lengths $l_i^2 = \hbar/(m\omega_i)$, these effects can be neglected. This result has two consequences.

(1) The dominant contribution for the diamagnetic shift comes from squeezing the wave function in the strong confinement (z) direction. All energy levels are expected to shift parallel in the magnetic field, since all electrons in this regime occupy the ground state ($n = 0$) of the ω_z potential. This means that the differences of Coulomb peak positions can safely be interpreted as a result of spin effects.

(2) The dependence of the Coulomb peaks as a function of parallel field is governed by the difference of the diamagnetic shifts in the source and drain with respect to the diamagnetic shift of the energy levels in the dot. These diamagnetic shifts are different because the 2D carrier density in the quantum dot, i.e., the Fermi energy in the dot, is reduced with respect to the leads. From the direction of the diamagnetic shift in our dot it follows that $\omega_z^{2\mathrm{DEG}}$ is smaller than ω_z^{dot}. By fitting parabolas to the observed Coulomb peak dispersion in Fig. 10 (see dashed line for peak starting at -4.52 V) we find a difference $\Delta z = \sqrt{\langle z_{2\mathrm{DEG}}^2 \rangle - \langle z_{\mathrm{dot}}^2 \rangle} = 3$ nm, a value that is reasonable if compared to simulations.

VII. DISCUSSION

In a single-particle picture, where the exchange interaction is neglected, one would expect that orbital states would be successively populated by spin-up and spin-down electrons. For our quantum dot we estimate interactions to be important, since the corresponding 2D density is low. In this case exchange interactions are expected to have a significant influence in maximizing the ground-state spin and values $s_N > 1/2$ can be expected.[9–11] In addition, it has been predicted[12] that only very few spin pairs occur in such a case. To our knowledge, the question of how the dot-lead coupling influences the sequence of ground-state spins in strongly interacting quantum dots has not been theoretically addressed.

Experimentally, the assumption that orbital effects play a minor role in the linear change in the Coulomb peak separation as a function of parallel field is on relatively safe grounds (see preceding section). Our data suggest that the linear behavior of the Coulomb peaks in $B_\parallel$ found in all coupling regimes is governed by Zeeman splitting according to Eq. (1). The extracted g factor is found to be similar to that of the bare value in bulk GaAs. Our experimental obser-

vations in the intermediate- and strong-coupling regimes agree qualitatively with the existing predictions for closed dots with strong interactions. Not only the observation of states, which move linearly in energy as a function of parallel field, but also the sequence of spin-up and spin-down single-electron states, not necessarily in sequential order, supports this view.

The combination of data taken as a function of both parallel and perpendicular magnetic fields for a quantum dot in the same state is a unique feature of our experiments. In the data, as a function of the perpendicular field, spin pairs can be assigned in agreement with the observations in parallel magnetic fields. The results give strong evidence for the predictions of the random matrix theory[12] describing the population of spin states in quantum dots for various strengths of interactions.

Possible sequences of ground-state spins have been determined, which agree with the statistical predictions for strongly interacting dots.[11] Occasionally, interactions in our system seem to be strong enough such that by the addition of an individual electron, the corresponding many-particle state exhibits $s_N \geq 1$ behavior.[29] The number of electrons in our dot changes by a factor of 2 in the investigated range of plunger gate voltage. Since the interaction parameter r_s is proportional to the inverse of the square root of the electron density, and the dot also increases its geometric size with increasing electron number, we can assume that r_s does not change much (probably less than 20%) within the investigated parameter range. It is therefore expected that the occurrence of higher spin states (such as $s_N = 1$) would not change much, and remain small but significant throughout the regimes. This agrees with the observations in the intermediate- and strong-coupling regimes.

In the weak-coupling regime the spin assignment in Fig. 5 is in agreement with the above arguments. The data indicate that several successive electrons occupy states with the same spin direction, which is an analogy of Hund's rules for atoms. The total spin of the dot may therefore take on values even larger than 1. However, the strong fluctuations in the peak positions make this analysis not as conclusive as in the other coupling regimes. It was previously observed[25] that the weak-coupling regime, which is naively expected to give the best results for the analysis of spin states, since the peaks are narrowest, does not prove itself very definitive for such investigations.

In the intermediate- and strong-coupling regimes, on the other hand, subsequent states of the dot seem to be less frequently occupied with parallel spins as compared to the weak-coupling regime. In the intermediate-coupling regime, the occurrence of spin pairs would therefore be more likely, in agreement with the peak correlations in the measured data for $B_\perp$. However, also in this regime the $B_\parallel$ data indicate that the total ground-state spin of the dot occasionally takes on values of at least $s_N = 1$. Although a precise determination of the spin of the dot cannot be uniquely reconstructed from the sequence of slopes, we find $s_N > 1/2$ only rarely.

In the strong-coupling regime the conductance peaks become wider and single-level transport cannot be achieved. This leads to a general enhancement of correlations in posi-

tion and amplitude between neighboring peaks. As far as spin pairs are concerned we were therefore only occasionally able to find neighboring peaks with correlations in $B_\perp$ significantly stronger than average. Trying to reconstruct possible sequences of ground-state spins from the measured data in $B_\parallel$ we come to realize that even in the strong-coupling regime one cannot avoid involving at least $s_N = 1$ states, although they occur infrequently.

The occurrence of three well-defined branches with slopes $\pm g\mu_B$ and 0 is not obvious in the strong-coupling regime. If transport through several levels with possibly different spins contributes to the position and amplitude of a given Coulomb-blockade peak, one would expect averaging of the corresponding Zeeman shifts. This would reduce the slope of peak separations as a function of in-plane field, similar to the effect of temperature.

It is worth mentioning that very rarely we observe two successive ascending or descending slopes in a plot of peak position differences vs magnetic field such as Fig. 6. A possible explanation of such an effect is that the ground-state spins of the $(N+1)$th electron dot and that of the Nth electron dot differ by more than 1/2, indicating that the arrival of the electron in the dot rearranges the spin orientation of other electrons.

Generally speaking we find that the spin behavior is more robust than expected from the involved energy scales. A similar statement was recently made by Glazman and co-workers in the context of the Kondo effect in strongly coupled dots in which charge quantization no longer occurs.[34]

VIII. CONCLUSIONS

The behavior of Coulomb-blockade peaks with magnetic fields applied in the plane of and perpendicular to quantum dots in semiconductor heterostructures has been investigated for a range of coupling regimes between the dot and its leads. In the weak-coupling regime the positions of the Coulomb-blockade resonances show strong fluctuations, which inhibit assignments of spin to a given state but are suggestive of large ground-state spin in the dot. In the intermediate-coupling regime, the experimental observations are in good agreement with predictions based on a single-particle transport scenario. This holds for magnetic fields applied parallel and perpendicular to the plane of the electron gas. In the strong-coupling regime the interpretation of the data still follows the single-level transport picture in parallel magnetic-field. However, some states show a stronger parallel magnetic field dependence as one would expect for weakly interacting $s=1/2$ particles with the bare g factor of GaAs. In both, the intermediate- and the strong-coupling regimes, total ground-state spins larger than 1/2 occur occasionally and spin pairs are rare. These findings are in good agreement with theoretical predictions for strongly interacting quantum dots.

*Present address: Fakultät für Physik, Universität Freiburg i.Br., 79104 Freiburg, Germany.

†Permanent address: Ludwig-Maximilians-Universität München, Theresienstr 37, 80333 München, Germany.

[1] M.A. Kastner, Rev. Mod. Phys. **64**, 849 (1992).

[2] For a review, see L. P. Kouwenhoven, C.M. Marcus, P.L. McEuen, S. Tarucha, R.M. Westervelt, and N.S. Wingreen, in *Mesoscopic Electron Transport*, edited by L.P. Kouwenhoven, G. Schön, and L.L. Sohn (Kluwer Academic, Dordrecht, MA, 1997).

[3] S. Tarucha, D.G. Austing, T. Honda, R.J. van der Hage, and L.P. Kouwenhoven, Phys. Rev. Lett. **77**, 3613 (1996).

[4] U. Sivan, R. Berkovits, Y. Aloni, O. Prus, A. Auerbach, and G. Ben-Yoseph, Phys. Rev. Lett. **77**, 1123 (1996).

[5] F. Simmel, T. Heinzel, and D. A. Wharam, Europhys. Lett. **38**, 123 (1997).

[6] S.R. Patel, S.M. Cronenwett, D.R. Stewart, A.G. Huibers, C.M. Marcus, C.I. Duruöz, J.S. Harris, K. Campman, and A.C. Gossard, Phys. Rev. Lett. **80**, 4522 (1998).

[7] S. Lüscher, T. Heinzel, K. Ensslin, W. Wegscheider, and M. Bichler, Phys. Rev. Lett. **86**, 2118 (2001).

[8] A. Fuhrer, S. Lüscher, T. Ihn, T. Heinzel, K. Ensslin, W. Wegscheider, and M. Bichler, Nature (London) **413**, 822 (2001).

[9] R. Berkovits, Phys. Rev. Lett. **81**, 2128 (1998).

[10] A.V. Andreev and A. Kamenev, Phys. Rev. Lett. **81**, 3199 (1998).

[11] P.W. Brouwer, Y. Oreg, and B.I. Halperin, Phys. Rev. B **60**, R13 977 (1999).

[12] H.U. Baranger, D. Ullmo, and L.I. Glazman, Phys. Rev. B **61**, R2425 (2000).

[13] P. Jacquod and A.D. Stone, Phys. Rev. Lett. **84**, 3938 (2000).

[14] S. Tarucha, D.G. Austing, Y. Tokura, W.G. van der Wiel, and L.P. Kouwenhoven, Phys. Rev. Lett. **84**, 2485 (2000).

[15] P. Hawrylak, C. Gould, A. Sachrajda, Y. Feng, and Z. Wasilewski, Phys. Rev. B **59**, 2801 (1999).

[16] R.C. Ashoori, H.L. Stormer, J.S. Weiner, L.N. Pfeiffer, K.W. Baldwin, and K.W. West, Phys. Rev. Lett. **71**, 613 (1993).

[17] A.S.G. Thornton, T. Ihn, P.C. Main, L. Eaves, and M. Henini, Appl. Phys. Lett. **73**, 354 (1998).

[18] A.C. Gossard, IEEE J. Quantum Electron. **22**, 1649 (1986).

[19] K.D. Maranowski, J.P. Ibbetson, K.L. Campman, and A.C. Gossard, Appl. Phys. Lett. **66**, 3459 (1995).

[20] G. Salis, B. Graf, K. Ensslin, K. Campman, K. Maranowski, and A.C. Gossard, Phys. Rev. Lett. **79**, 5106 (1997).

[21] S. Lindemann, T. Ihn, T. Heinzel, K. Ensslin, K. Maranowski, and A.C. Gossard, Physica E (Amsterdam) **13**, 638 (2002).

[22] P.L. McEuen, E.B. Foxman, J. Kinaret, U. Meirav, M.A. Kastner, Ned S. Wingreen, and S.J. Wind, Phys. Rev. B **45**, 11 419 (1992).

[23] F. Simmel, D. Abusch-Magder, D.A. Wharam, M.A. Kastner, and J.P. Kotthaus, Phys. Rev. B **59**, 10 441 (1999).

[24] D.S. Duncan, D. Goldhaber-Gordon, R.M. Westervelt, K.D. Maranowski, and A.C. Gossard, Appl. Phys. Lett. **77**, 2183 (2000).

[25] J.A. Folk, C.M. Marcus, R. Berkovits, I.L. Kurland, I.L. Aleiner, and B.L. Altshuler, Phys. Scr., T **90**, 26 (2001).

[26] E.B. Foxman, P.L. McEuen, U. Meirav, N.S. Wingreen, Y. Meir, P.A. Belk, N.R. Belk, M.A. Kastner, and S.J. Wind, Phys. Rev. B **47**, 10 020 (1993).

[27] A.A.M. Staring, B.W. Alphenaar, H. van Houten, L.W. Molenkamp, O.J.A. Buyk, M.A.A. Mabesoone, and C.T. Foxon, Phys. Rev. B **46**, 12 869 (1992).

[28] G. Salis, Y. Kato, K. Ensslin, D.C. Driscoll, A.C. Gossard, and D.D. Awschalom, Nature (London) **414**, 619 (2001).

[29] L.P. Rokhinson, L.J. Guo, S.Y. Chou, and D.C. Tsui, Phys. Rev. B **63**, 035321 (2001).

[30] M. Ciorga, A.S. Sachrajda, P. Hawrylak, C. Gould, P. Zawadzki, S. Jullian, Y. Feng, and Z. Wasilewski, Phys. Rev. B **61**, R16 315 (2000).

[31] Y. Alhassid, Rev. Mod. Phys. **72**, 895 (2000).

[32] W. Beinvogl, A. Kamgar, and F. Koch, Phys. Rev. B **14**, 42 274 (1976).

[33] K. Ensslin, A. Wixforth, M. Sundaram, P.F. Hopkins, J.H. English, and A.C. Gossard, Phys. Rev. B **47**, 1366 (1993).

[34] L.I. Glazman, F.W.J. Hekking, and A.I. Larkin, Phys. Rev. Lett. **83**, 1830 (1999).